Available online at www.sciencedirect.com
ScienceDirect
Biochimica et Biophysica Acta 1767 (2007) 353–361
Biochimica et Biophysica Acta
BBA
www.elsevier.com/locate/bbabio

Macromolecular crowding and its influence on possible reaction mechanisms in photosynthetic electron flow

I.G. Tremmel [a,*], E. Weis [c], G.D. Farquhar [b]

[a] Max-Planck-Institute for Biophysical Chemistry, Theoretical and Computational Biophysics Department, Am Fassberg 11, D-37077 Goettingen, Germany
[b] Department of Environmental Biology, Research School of Biological Sciences, Australian National University, Canberra, A.C.T. 2601, Australia
[c] Institut für Botanik, Westfälische Wilhelms-Universität Münster, Schloßgarten 3, D-48149 Münster, Germany

Received 30 September 2006; received in revised form 27 February 2007; accepted 1 March 2007
Available online 19 March 2007

Abstract

The diffusion of plastoquinol and its binding to the *Qo* site of the cyt *bf* complex in the course of photosynthetic electron transport was studied by following the sigmoidal flash-induced re-reduction kinetics of P700 after previous oxidation of the intersystem electron carriers. The data resulting from these experiments were matched with a simulation of electron transport using Monte Carlo techniques. The simulation was able to account for the experimental observations. Two different extreme cases of reaction mechanism at the *Qo* site were compared: a diffusion limited collisional mechanism and a non-diffusion limited tight binding mechanism. Assuming a tight binding mechanism led to best matches due to the high protein density in thylakoids. The varied parameters resulted in values well within the range of published data. The results emphasise the importance of structural characteristics of thylakoids in models of electron transport.

Keywords: Photosynthesis; Thylakoid membranes; Macromolecular crowding; Reaction mechanism; Plastoquinone diffusion; Monte Carlo simulation

1. Introduction

Photosynthetic electron flow involves the integral complexes of photosystem II, cytochrome *bf*, and photosystem I that operate in series via the mobile carriers plastoquinone and plastocyanin. In principle the problem of electron transport between PS II and cyt *bf* is equivalent to that of ubiquinol diffusion and its oxidation at the cytochrome bc_1 complex in bacterial and mitochondrial electron transport. However, in thylakoids of higher plants the two photosystems are laterally separated. PS II is located in the grana core whereas PS I is located in the grana margins and the stroma lamellae [1–6]. As a consequence diffusing electron carriers, transporting electrons between the photosystems and cyt *bf* are required to travel distances of up to 200–250 nm between the centre of the grana and the margins. The two mobile carriers, plastoquinone and plastocyanin, are both diffusible carriers found throughout the thylakoids. There is no general agreement on which is responsible for long range transport.

Plastocyanin is a small water-soluble protein that carries its redox group well protected within the protein matrix whereas plastoquinol is a small lipid-soluble molecule that transports electrons on its surface. PQ has a high diffusion coefficient. Because of this it has been the favourite candidate for the long range mobile carrier [5].

Most published models of electron transport assume a common plastoquinone pool shared by all PS II (one model considering possible consequences of thylakoid architecture on electron transport is the model of Mitchell and co-workers [15]). A shared plastoquinone pool implicitly assumes fast plastoquinone exchange throughout the membrane. However, evidence was found against the notion of a common plastoquinone pool shared by PS II in the grana and those in the stroma thylakoids [7]. Furthermore, one has to take into account that the membrane in which it is diffusing is crowded with proteins that may act as obstacles (see e.g. [8–12]). The first evidence for this arose from estimations of the diffusion coefficient for PQ in phosphatidylcholine lipid vesicles [13]. More recent measurements in thylakoids using fluorescence quenching of pyrene yielded a coefficient between 0.1 and 3×10^{-9} cm^2/s, which is 100 times smaller than the coefficient in artificial lipid vesicles

* Corresponding author.
E-mail address: ira@germanynet.de (I.G. Tremmel).

0005-2728/$ - see front matter © 2007 Elsevier B.V. All rights reserved.
doi:10.1016/j.bbabio.2007.03.007

without proteins [14]. Particularly long range diffusion of plastoquinone in thylakoids may be severely restricted by the integral proteins. Further, it has been shown that such restricted diffusion may strongly influence kinetic rates [16–18] and the time course of enzymatic reactions [19].

High concentrations of background macromolecules that do not participate directly in a particular considered reaction, like e. g. LHC II in electron transport, have been observed to induce order-of-magnitude or larger changes in the rates and equilibria of numerous investigated reactions [20] (for reviews on molecular crowding see e. g. [21,17,18,22,23]). However, the contribution of crowding and diffusion limitation to reaction kinetics of electron transport is not only determined by the degree of crowding and the apparent diffusion coefficient of plastoquinol but also by the reaction mechanism (see also [20,17,16,22]). Thus it is necessary to investigate the effects of crowding on a biochemical reaction for each special case taking into account the specific features of the system. Therefore in the present work electron transport was modelled using a Monte Carlo approach incorporating realistic protein densities and shapes. The complexes consist of PS II with tightly bound LHC II [24], cyt *bf* [25], and free LHC II [26] randomly distributed within the membrane (see also [11]). Plastoquinone diffuses between these integral proteins. For the binding mechanism two hypothetical extreme cases were investigated, tight binding and a collisional mechanism. The tight binding mechanism includes an irreversible binding of PQ to the Q_o site of cyt *bf* before its slow oxidation takes place. The collisional mechanism implies immediate electron transfer after a successful encounter (see also [15]). Both mechanisms lead to an exponential decay with the same rate constant k when diffusion processes are not limiting. In thylakoids however, where diffusion may be highly restricted, the two mechanisms were expected to lead to different behaviours. Therefore both mechanisms were tested with the model and the results compared.

The experimental approach to the role of the diffusion of plastoquinol was to follow the re-reduction of P700, the reaction centre chlorophyll of PS I, by electrons induced by a flash at PS II. This is a convenient method of accurately measuring whole-chain electron transport. The rate constant of the sigmoidal reduction kinetics and the initial lag give information about the rate-determining oxidation of plastoquinol [27] and reactions preceeding this step [28], respectively.

The experimental data obtained were then compared with the results of the simulation. The measured data were matched by varying rate constants used in the simulation. A similar approach was chosen by Mitchell and co-workers [15]. Electron transfer at cyt *bf* was modelled according to an obligatory Q-cycle as described in Methods.

2. Methods

2.1. Isolation of thylakoids from spinach

Leaves of 6 to 8 weeks old spinach (*Spinacea oleracea* var. polka) were used for the preparations. The plants were grown hydroponically at about 13-16 °C with nutrients according to Randall and Bouma [29]. The illumination period was 10 h and light intensity (400–700 nm) was about 200 μmol photons m^{-2} s^{-1}. Care was taken that only leaves not shaded by others were used. Intact chloroplasts were isolated as described in [30]. Leaves of spinach were harvested at the end of the dark period to minimize their starch content. Thylakoids were freshly prepared from chloroplasts before every series of measurements. To obtain thylakoids, chloroplasts were shocked osmotically: chloroplasts were placed in hypotonic assay buffer (7 mM $MgCl_2$, 80 mM KCl, 30 mM HEPES, typical dilution of thylakoid suspension to buffer solution: 1:75). After 60 s an equal amount of hypertonic assay buffer (7 mM $MgCl_2$, 80 mM KCl, 30 mM HEPES, 600 mM Sorbitol) was added to obtain an isotonic assay medium. Chlorophyll concentration was usually 10–20 μg/ml. This treatment leaves the thylakoid membrane system quite intact (as indicated by an extremely low proton leakage when protonmotive force is built up [31]). Typical whole chain electron transport rates were 1150 μmol_{e-} h^{-1} mg_{chl}^{-1} (287 $mmol_{e-}$ s^{-1} mol_{chl}^{-1}). PS II activity was usually around 2300 μmol_{e-} h^{-1} mg_{chl}^{-1} (573 $mmol_{e-}$ s^{-1} mol_{chl}^{-1}).

2.2. P700 re-reduction

The flash-induced kinetics of P700 re-reduction were measured between 820 and 870 nm with the Dual-Wavelength Emitter-Detector Unit (ED-P700DW, Heinz Walz GmbH, Effeltrich, Germany) in combination with a standard PAM Chlorophyll Fluorometer (PAM 101, Heinz Walz GmbH, Effeltrich, Germany). Saturating light flashes were applied with a single turnover flash lamp (XST-103, Heinz Walz GmbH, Effeltrich, Germany). Continuous weak far-red light of ca. 17 W/m^2 ensured that all the components between the two photosystems were oxidised between flashes. The background light was checked to ensure that it did not measurably increase the amount of oxidised P700. Twenty flashes were applied to the same sample and averaged. This was repeated with the same sample 6–7 times (e.g. 120–140 flashes). A time of 5 s between two measurements allowed for relaxation of the samples. The responses to averaged 20 flashes were then checked for ageing effects. Usually measurements of up to 100 flashes did not show significant ageing. The measurements were repeated with a fresh sample and another series of flashes applied. To obtain the data that were matched with the model the kinetics of three different samples were averaged. The frequency of data acquisition was 25000 Hz.

The data acquisition and triggering was carried out with the help of a LabVIEW-program (Laboratory Virtual Instrument Engineering Workbench, version 6.1, Copyright 2000 National Instruments Corporation). For the measurements a commercially developed program (von Kruedener und Danckwerts Meß-und Prüfsysteme, Kürten, Germany) was modified and further tailored to the measurements described in the present work.

Thylakoids were obtained by osmotically shocking chloroplasts. This procedure might lead to dilution of ferredoxin and in consequence to recombination between $P700^+$ and reduced FeS acceptors in PS I. To check whether such recombination might influence our experiments we carried out additional experiments with DCMU. If a recombination between $P700^+$ and FeS acceptors does not occur one would expect no decay of $P700^+$ when electron transport from PS II is blocked by an inhibitor like DCMU. The P700 re-reduction with and without DCMU is shown in Fig. 1. In the presence of DCMU during the first 10 ms a decay of only about 5% of the $P700^+$ could be observed.

2.3. The simulation

The basic simulation was similar to that described in [11]. However, the protein-objects were now extended to include binding sites for redox reactions. Similarly the plastoquinone (PQ)-objects were extended to have a state, reflecting their redox state. Only excluded volume interactions between the particles were considered.

2.4. The protein-objects

Accounting for the dimeric character of PS II and cyt *bf* each protein-object has a double set of binding sites. Due to the grid character of the simulation, the resolution was restricted to the distance between two grid points (i.e. 1 nm). Therefore the binding sites may be shifted somewhat relative to the body of the protein for different orientations of the protein within the thylakoids. To avoid a binding site becoming located within the protein itself the binding site was

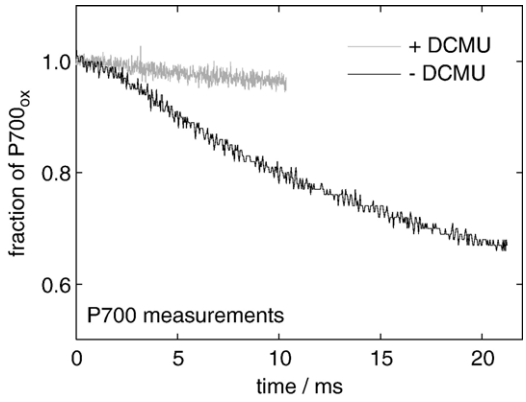

Fig. 1. Observed P700 re-reduction in thylakoids as described in Methods (−DCMU). Experiments with DCMU were carried out to check whether recombination between $P700^+$ and reduced FeS acceptors influences our measurements.

calculated as a floating point parameter for each orientation of the protein. Given this floating point number, the next neighbouring grid point not occupied by the protein itself was chosen to represent the binding site. The two binding sites of each cyt *bf* -monomer, Q_o and Q_r, are very close to each other. Therefore, the determination of binding sites in this manner may lead to a situation where both binding sites, Q_o and Q_r, are placed on the same site of the grid. This was avoided by choosing the second nearest neighbour on the grid to represent the binding site if the determination of a Q_r binding site resulted in a grid point that was already occupied by Q_o.

2.5. The plastoquinone-objects

The plastoquinone-objects were similar to the tracers used in [11]. Unlike the tracers, PQ cannot occupy the same vacant site on the grid. Furthermore the PQ-objects were extended by the attribute 'state' that accounts for the different redox states of PQ. Each PQ can be in three states: oxidised, one-fold reduced and two-fold reduced. Only oxidised and two-fold reduced plastoquinone were allowed to move. This takes into account that no free semiquinone is found in thylakoids. It reflects the finding that the dissociation constant of oxidised PQ as well as that of PQH_2 (i.e. two-fold reduced) is ca. three orders of magnitude higher than that of the singly reduced semi-quinone [32]. This may be caused by Coulomb interactions that stabilize the semiquinone at the Q_B site, whereas the neutral forms (PQ and PQH_2) may leave the binding site easily.

2.6. Modelling electron transport

At each encounter between PQ and a binding site of PS II or cyt *bf* first a test was carried out to ascertain whether PQ and the binding site were both in the right redox state (e.g. PQ oxidised at an encounter with Q_B, and Q_B carrying an electron). The next test was for whether the electron was then actually transported. The rate constants of the single reactions were taken as the probability, p, for a reaction to take place. At an encounter between PQ and a binding site (both in the right redox state) a random number, r, between zero and one was chosen. If $r<(1-p)$, the electron was not transferred. Consequently, the smaller the value of p, the higher the probability of choosing a number that satisfies the condition and thus the electron was not transferred. A probability $p=0$ always satisfies the condition and electron transport was not carried out. In turn, a probability $p=1$ does not fulfill the condition and the transfer was always carried out. Assuming high availability of the reactants and no diffusion limitations, as is the case for ideal *in vitro* experiments, this behaviour results in an exponential decay corresponding to the rate constant (p).

As long as the sample was illuminated, Q_A was assumed to always carry electrons ready for transfer at a successful encounter (i.e. saturating light conditions).

For the electron transfer at cyt *bf* an obligatory Q-cycle was assumed [33–37]. If FeS was oxidised and PQ two-fold reduced, electron transfer to FeS at the Q_o binding site was carried out after a successful encounter. After successful electron transfer to FeS the transfer of the second electron of the plastoquinol to cyt b_l followed immediately if the latter was oxidised [38,39]. If cyt b_h was oxidised, the electron was immediately transferred from cyt b_l to cyt b_h [38]. For the sake of simplicity the oxidation of PQH_2 at the Q_o site was assumed to have the same rate constant regardless of whether there was reduced cyt *b* on the cyt *bf* complex.

If an oxidised PQ encountered the Q_r site, an electron was transferred from cyt b_h to PQ if the encounter was evaluated to be successful. The now singly reduced PQ was not allowed to move and it stayed at the Q_r binding site until the second electron transfer took place. This was the case when cyt b_h was reduced again and if the encounter was evaluated to be successful according to the rate constant for electron transfer at the Q_r site. The rate constant for both electron transfers was assumed to be the same, regardless of whether PQ was oxidised or singly reduced.

Electron transport between the Rieske-centre (FeS) and P700 was treated as a 'black-box' and one equilibrium constant was used to describe the redox state of FeS and P700.

2.7. Data fitting

The simulation allows certain parameters to vary in order to match experimental data on redox experiments. Parameters that may be varied are the rate constants of the following reactions:

$$QA^- + QB \xrightarrow{k_0} QA + QB^- \quad \text{transfer of first electron,}$$

$$QA^- + QB^- \xrightarrow{k_1} QA^- + QB^{2-} \quad \text{transfer of second electron,}$$

$$PQH_2 + FeS_{ox} \xrightarrow{k_3} PQ^- + FeS_{red} + 2H^+ \quad \text{oxidation of } PQH_2 \text{ at } Q_o,$$

$$PQ + \text{cyt } b_h^- \xrightarrow{k_4} PQ^- \quad \text{reduction of PQ at } Q_r,$$

$$FeS_{red} + P700^+ \overset{K_5}{\leftrightarrow} FeS_{ox} + P700 \quad \text{equilibrium,}$$

and k_2 is the dissociation of plastoquinol. The rates of electron transfer at the Q_B binding site are reasonably well known. Therefore, the rate constants for the first (k_0) and the second electron transfer (k_1) at PS II were chosen to be 6670 and 2500 s^{-1}, respectively. These values are within the range of those given by Diner and co-workers [40]. Assuming free plastocyanin diffusion the equilibrium constant K_5 can in principle be calculated from the equilibrium constants for the following reactions:

$$FeS_{red} + \text{cyt } f_{ox} \overset{K_a}{\leftrightarrow} FeS_{ox} + \text{cyt } f_{red}$$

$$\text{cyt } f_{red} + PC_{ox} \overset{K_b}{\leftrightarrow} \text{cyt } f_{ox} + PC_{red}$$

$$PC_{red} + P700^+ \overset{K_c}{\leftrightarrow} P700 + PC_{ox}.$$

However, values for K_a, K_b, and K_c as found in the literature, vary greatly. For K_a values can be found between 3.2 [41] and 18 [42]. Values for K_b vary between 1.0 [43] and 10 [44,38]. Finally, values for K_c range from 5 [45] to 87 [46]. This yields a range of values for K_5 from 16 to 15660. A collection of references to these equilibrium constants can be found in Berry and Rumberg [47]. Nevertheless, the redox state of P700 only declines to ca. 80% (i. e. $P_{700}/P^+_{700}<0.25$) during the first 10 ms. Therefore, electrons will nearly always (99.8%) be transferred from the Rieske centre to P700 if the equilibrium constant K_5 is larger than about 150, since $P_{700}/P^+_{700}/K_5<0.002$.

The remaining free parameters (k_2, k_3, k_4) were varied to find the function that leads to the least sum of errors squared when compared with the experimental data. k_2 was allowed to vary between 200 and 5000 s^{-1}, k_3 between 100 and 100000 s^{-1}, and k_4 between 100 and 100000 s^{-1}.

Two different algorithms were used to vary the parameters: a genetic algorithm and an algorithm according to Powell [48]. Genetic algorithms, when properly implemented, are capable of both exploration (broad search) and exploitation (local search) of the search space. They are particularly useful if the function to be optimised has several optima. In this case a classical algorithm such as Powell's may get trapped in a local optimum instead of finding the global optimum. However, genetic algorithms are relatively slow. Thus it is convenient to combine both approaches.

The implementation of the Powell-routine is described in [49]. In the present work an algorithm was used that enabled the choice of intervals within which the varied parameters were changed. This extension of Powell's algorithm was kindly developed by Thomas Strauß.

2.7.1. Genetic algorithm to do optimisation

A genetic algorithm creates a population of solutions based on the fitting-parameters. The algorithm then operates on the population to evolve the best solution. All fitting-parameters together build a chromosome where each single fitting-parameter relates to a gene. The genetic algorithm determines which individuals should survive, which should reproduce, and which should die (see Fig. 2). This relates to the fitness of an individual, which in turn corresponds to the sum of errors squared (the larger the sum of the errors squared the less fit). Typically a genetic algorithm has no obvious stopping criterion. Often the number-of-generations is used as a stopping measure. Other typical stopping criteria are the fitness-of-best-individual or convergence-of-population.

For the problem addressed here the 'steady-state genetic algorithm' was chosen. It uses overlapping populations with a user-specifiable amount of overlap.

The algorithm creates a population of individuals. In each generation the algorithm creates a temporary population of individuals, adds these to the previous population, then removes the worst individuals in order to return the population to its original size. The amount of overlap between generations can be chosen by specifying a replacement parameter. Newly generated offspring were added to the population, then the worst individuals were destroyed (so the new offspring may or may not make it into the population, depending on whether they were better than the worst in the population).

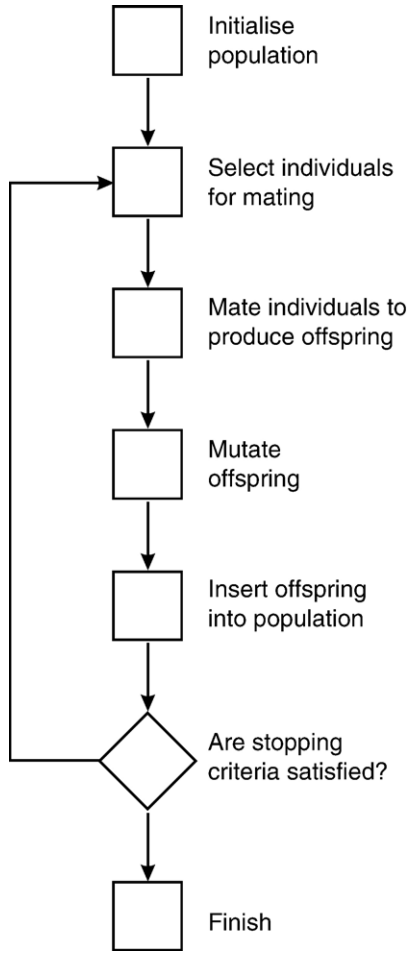

Fig. 2. Schematic diagram of the genetic algorithm.

2.8. Starting conditions and settings

The stoichiometries used were the ones calculated in [11]: PS II : cyt *bf* : LHC II=2.56 : 1 : 14.12. Additionally two PS I (monomers) per PS II (dimer) were assumed. The acceptors of PS II function as a two-electron gate. Therefore under steady-state conditions one half of the acceptors will stay as a semiquinone at the Q_B site on PS II after a saturating light flash while the other half produces PQH_2. Accordingly every second QB site (randomly chosen) has a bound PQH_2 that is released after dissociation has taken place. No free diffusing oxidised PQ was modelled to save computing time. However, free, diffusing PQ was not expected to act as an obstacle to PQH_2 migration or have any other significant influence. For cyt *bf* it was assumed that the state with one reduced cyt *b* is stable within the measuring time. This is in agreement with the observation that one quarter of cyt *b* is reduced in the steady-state (note that each cyt *bf* contains two cyt *b*) [50]. The other components are oxidised before the flash [51].

Since calculation and fitting of the curves are computationally demanding and take a long time, only the first 10 ms of the measured curve, the most interesting part regarding the diffusion of PQ, was fitted.

3. Results

P700 re-reduction was measured to investigate whole-chain electron transport (Fig. 1). To obtain quantitative information about rate constants involved in photosynthetic electron transport, rate constants used in the model were varied to match the experimental data. Two different mechanisms at the Q_o site on cyt *bf* were compared: tight binding and a collisional mechanism.

Parameters that were varied are k_2 (dissociation of PQH_2 from PS II), k_3 (PQH_2 oxidation at Q_o), and k_4 (PQ reduction at Q_r) (as described in Methods). Other rate constants involved are reasonably well known and therefore these values were not varied but taken from the literature.

3.1. Tight binding mechanism

For the tight binding mechanism an irreversible tight binding of PQ at the Q_o site of cyt *bf* was assumed followed by the slow oxidation of PQ.

Assuming there is a tight binding mechanism, a good fit to the measured data could be obtained (see Fig. 3). An occupied area fraction of 0.70 was chosen corresponding to the value estimated for grana thylakoids in [52,11]. For the conditions used in the simulation, this area fraction is above the percolation threshold and hence diffusion domains bounded by the integral photosynthetic proteins are formed. PQ can diffuse more or less freely within these diffusion domains but cannot leave them [11].

The parameters resulting in the best fit were well within the range of published data measured on thylakoids (see Table 1). The lattice size was chosen to be 400 nm × 400 nm (with periodical boundary conditions). This size corresponds to the size of the grana core. The lattice size was relatively large and inhomogeneities caused by the random distribution of the proteins should be minimised. However, the exact values of the rate constants depended on the configuration of the proteins. Three different random protein configurations were investigated and parameters varied to match the measured data (see Table 2).

Interestingly the different parameters varied to a different extent. Whereas k_3 was within a small range for all configura-

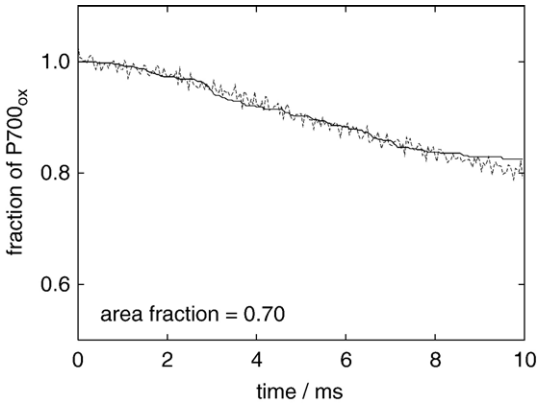

Fig. 3. Comparison of the simulation (solid line) with the observed P700 re-reduction (dashed line) for a tight binding mechanism. An occupied area fraction of 0.70 (i.e. above the percolation threshold) was assumed. Rate constants were k_2=1206 s^{-1}, k_3=295 s^{-1}, and k_4=335 s^{-1} (nomenclature as described in Methods).

tions investigated k_4 varied to a great extent. This is not entirely unexpected since k_3 describes the oxidation of PQH_2 at the Q_o site on cyt *bf* which is agreed to be the slowest step of whole chain electron transfer. Thus electron flux was expected to be very sensitive to this parameter. k_4 describes the reduction of PQ at the Q_r binding site on cyt *bf*. It does not seem to play a major role in determining the measured curve. This was probably due to the low probability of a PQ finding a cyt *bf* carrying two electrons when only one saturating light flash was applied. Consequently the simulation was not expected to be very sensitive to this parameter.

To investigate the influence of the protein density and hence the retardation of PQ migration, the simulation was repeated for an occupied area fraction of 0.60, which is below the percolation threshold.

As with an area fraction of 0.70 good fits were obtained (see Fig. 4). However, the rate constants obtained were not in good agreement with published data. To match the experimental data the reaction at the Q_o site would need to be very slow (k_3=100 s^{-1}, the lowest value allowed in the simulation). This is probably to compensate for the much faster 'finding' of the binding site due to the less restricted diffusion of PQ.

To elucidate the effect of restricted PQH_2 diffusion a hypothetical extreme case was also investigated (Fig. 5): an area occupation of 0.70 was chosen but it was assumed that the proteins do not interfere with PQ diffusion (i.e. that they are

Table 1
Rate constants for several electron transfer steps from literature and obtained from simulations

Rate constant in s^{-1}	Literature data	Reference	Area occupation		
			0.70	0.60	0.70 (permeable)
k_2	495–2310	[15]	1206	1641	243
	1000	[60]			
k_3	305	[38]	295	100	100
	200–330	[61,62]			
k_4	400	[38]	335	250	369

Table 2
Rate constants resulting from best fits for different random protein distributions with an area fraction of 0.70.

Rate constant	Different runs		
k_2	1206	725	1298
k_3	295	329	289
k_4	335	544	100

permeable to PQ). For PQH_2 oxidation the same rate constant (k_3) was obtained as for 0.60 area occupation (see Table 1). Additionally a slow dissociation from PS II (k_2) was obtained in the simulation (>4 ms) to account for the measured slow decline in the amount of oxidised P700. However, as can be seen in Fig. 5, the simulation does not match the experimental data well. At short times the simulated curve declines too slowly.

The initial lag (about 2 ms) before the steeper decline in the amount of oxidised P700 starts, may be caused by reactions preceding the oxidation of PQH_2 [15] (i.e. dissociation and diffusion of PQH_2 and possibly time spent at the Q_o site before being oxidised). Fig. 5 illustrates that this initial lag would be much too pronounced if the dissociation constant were as low as the one obtained in the simulation with proteins not restricting PQ migration.

3.2. Collisional mechanism

In the collisional mechanism it is assumed that electrons are transferred immediately at a successful encounter. The reaction constant determines the probability of an encounter being successful. This mechanism reflects a more diffusion limited scenario compared to the tight binding mechanism.

In this part a collisional mechanism was assumed instead of the tight binding mechanism. As can be seen in Fig. 6 good fits were obtained. However, the resulting rate constant for oxidation of PQH_2 at the Q_o site (k_2) was more than two orders of magnitude larger than that found in the literature for thylakoids (see Table 1). Accordingly the simulation predicts that a collisional mechanism would require rate constants for isolated complexes that are about 100-fold higher than those measured on thylakoids.

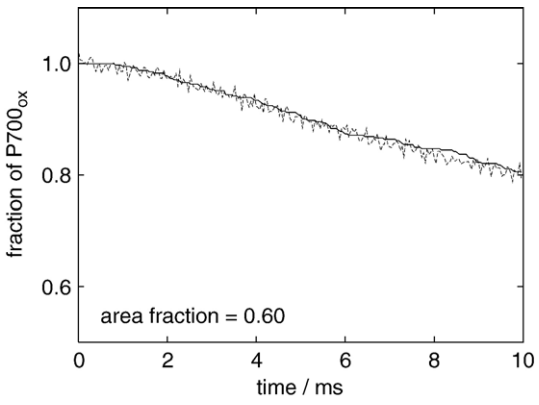

Fig. 4. As Fig. 3 but assuming an occupied area fraction of 0.60 (i.e. below the percolation threshold). Rate constants were k_2=1641 s^{-1}, k_3=100 s^{-1}, and k_4=250 s^{-1} (nomenclature as described in Methods).

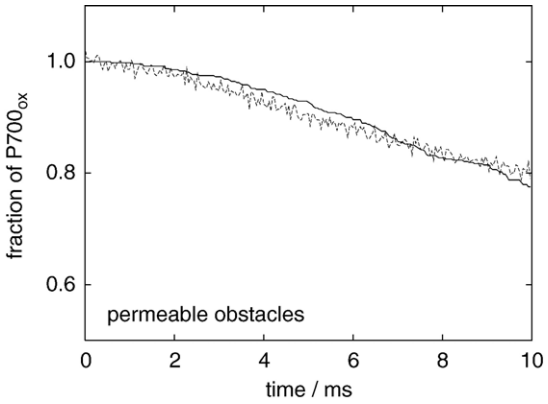

Fig. 5. As Fig. 3 but here the proteins were assumed to be permeable to PQ. Rate constants were k_2=243 s^{-1}, k_3=100 s^{-1}, and k_4=369 s^{-1} (nomenclature as described in Methods).

Similar investigations were carried out for an occupied area fraction of 0.60 and proteins that do not interfere with PQ diffusion (permeable) but it was not possible to match the data with reasonable rate constants (data not shown).

4. Discussion

Detailed knowledge of a great deal of rate constants of photosynthetic electron transport in thylakoids is available. Despite this, the mechanism of how the electrons are actually transferred is in many cases still unknown.

In the case of restricted diffusion it has been shown that depending on the reaction mechanism molecular crowding may induce order-of-magnitude or greater changes in rates and equilibria of reactions [20]. This may also be the case in thylakoids where about 70% of the space is occupied by proteins [52,11]. Restricted diffusion together with impeded mixing of the substrate, i. e. PQ, may severely influence reaction constants [19,17,18]. However, in some photosynthetic bacteria such as *Blastochloris viridis* or *Rhodospirillum rubrum* light harvesting complex 1 (LH1) form closed rings surrounding the reaction centre (RC) [53–55] and it is still under debate whether this hampers diffusion of ubiquinol to the RC. Comayras and co-workers [56] only found a moderate effect of such a barrier on turnover rates in the PufX− mutant of *Rhodobacter sphaeroides* that displays closed rings of LH1. Comayras and co-workers arrived at the conclusion that crowding of membrane proteins is not the main reason for restricted diffusion of quinone within the membrane. They propose that confinement of quinone is rather associated with the formation of quinone-rich regions around proteins as RCs or cyt bc complexes. However, it is not clear how quinones are distributed within the membrane and whether their distribution is the same in bacteria and higher plants. Proteins and their organisation in thylakoids of higher plants differ considerably from those in bacteria. In higher plants the two photosystems are separated which leads to the requirement of PQ diffusion across the membrane over distances of more than 200 nm after taking up two electrons at PS II. Furthermore, there is evidence that in higher plants diffusion of PQ is severely slowed [13,14]. Of course this could also be due to the formation of a quinone-rich phase within the lipid membrane but today there is no evidence for such phases in higher plants.

P700 re-reduction was measured and the data were matched with a simulation of the thylakoid membrane using best fits. In a crowded membrane it is possible to distinguish between reaction mechanisms that are indistinguishable in dilute media. We investigated two hypothetical extreme cases of reaction mechanisms of the electron transfer at the Q_o site on cyt *bf*: a diffusion limited collisional mechanism, where electron transfer takes place immediately at a successful encounter and a tight binding mechanism where PQ binds irreversibly before its slow oxidation takes place.

In summary, the experimental data were best matched when restriction of plastoquinone diffusion was pronounced (area fraction 0.70) and a tight binding mechanism was assumed. Lower area occupations or the assumption that proteins do not act as obstacles to PQ diffusion did not agree with published data on reaction constants. In these cases the rate constants obtained in the simulation (reflecting isolated complexes) were much slower than those taken from literature measured on thylakoids. This is in contradiction with the expected deceleration of rate constants in crowded membranes like thylakoids.

4.1. Rate constants in a crowded membrane

Our results clearly point out the importance of structural characteristics of thylakoids in models of electron transport. An influence of diffusion processes on reaction rates is also reported for the activation of transducin by rhodopsin [57]. Higher concentrations of reactants are expected to lead to a decreased rate of reaction by lowering the diffusion coefficient of the reactants (here only PQH_2 was considered to be mobile but this does not alter the principal results). On the other hand, they also lead to an increased reaction rate by the law of mass action. The law of mass action, however, relies on strict assumptions concerning, for instance, the characteristics of the reaction medium, which must be dilute, perfectly-mixed, and

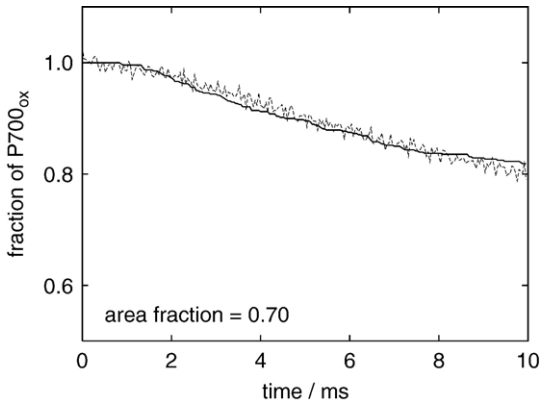

Fig. 6. Comparison of the simulation (solid line) with the observed P700 re-reduction (dashed line) for a collisional mechanism. An occupied area fraction of 0.70 (i.e. above the percolation threshold) was assumed. Rate constants were k_2=1352 s^{-1}, k_3=48800 s^{-1}, and k_4=49562 s^{-1} (nomenclature as described in Methods).

homogeneous [19]. These conditions are certainly not fulfilled in a membrane close to the percolation threshold where diffusion of PQ is severely restricted.

In a crowded membrane the apparent rate constant becomes fractal and decreases with time according to $k(t)=k(0)t^{-h}$ for $t\rightarrow\infty$ with the fractal kinetics exponent h [58]. The classic Michaelis–Menten formalism is thus a special case of a fractal reaction that corresponds to $h=0$. The time dependence of the reaction constant increases with increasing obstacle densities [19].

Towards the end of the measured time range a diminished rate of P700 re-reduction may be seen in Fig. 1. This slowing might be caused by a progressive decrease of reaction rates caused by the fractal effect. Accordingly, also all simulations with an occupied area fraction of 0.70 show a slightly slowed re-reduction towards the end of the simulated time range. Compared to the measurements slowing is more pronounced for the simulations. However, the measured re-reduction of P700 might be slightly overestimated due to recombination between $P700^+$ and reduced FeS acceptors in PS I (less than 5% as may be seen in Fig. 1). Interestingly, the rate of P700 re-reduction is diminished stronger for the collisional mechanism, which is in line with the stronger effect of crowding on diffusion limited reactions. Concordantly, the simulation assuming proteins as permeable to PQ diffusion does not show slowing of P700 re-reduction and hence cannot match the experimental data.

It has to be noted that the rate constants used in our simulation do not reflect the overall apparent rate constant but rather the probability for each single reaction to take place at a certain timestep. This is comparable to the rate constant in dilute media.

4.2. Collisional mechanism — a diffusion limited reaction

Experimental data could also be matched under the assumption of a collisional mechanism and an occupied area fraction of 0.70. However, in this scenario the simulation predicts rate constants of reactions on isolated complexes ($k_3=48800\ s^{-1}$) that are at least two orders of magnitude faster than those measured in thylakoids ($k_3=305\ s^{-1}$). This seems unlikely since rate constants for the reactions at the Q_o site on cyt *bf* measured on *Chlamydomonas reinhardtii in vivo* and *in vitro* are very similar [59].

The required fast reaction constant in the simulation can be explained by the diffusion limitation. In the case of diffusion limitation the rate constant in the simulation was composed of the probability of finding a binding site (diffusion limited) times the probability (k_i) for an electron transfer to take place (see also [21,20]). The value for k_3 found in the simulation however, refers to the rate of the actual electron transfer. To match the rate constants found in the literature ($305\ s^{-1}$) this would require a probability of about 1:160 for a PQH_2 to meet a Q_o binding site compared to the dilute case. Further, if a collisional mechanism were indeed the case, it is expected that the k_3-value for the actual electron transfer at the Q_o binding site found here ($k_3=48800\ s^{-1}$) would equal that measured *in vitro* where no diffusion limitation occurs. This however was not the case. The rate constant found in *C. reinhardtii* is 250–300 s^{-1} [59] and thus is within the same order of magnitude as the *in vivo* rates. Equal rates *in vivo* and *in vitro* would fit better with the tight binding mechanism (reaction limited and not diffusion limited).

It should be noted that in the case of a collisional mechanism the resulting rate constants were much more sensitive to the protein configurations than in the case of the tight binding mechanism. A factor of two was found for different starting conditions (not shown). Due to the diffusion limitation it was important whether or not a PQH_2 had good access to a Q_o binding site. However, rate constants resulting from other configurations were still not satisfying.

4.3. PQ oxidation at the Q_o site of cyt bf in a heavily crowded membrane is expected to be reaction limited rather than diffusion limited

In summary it seems that a collisional mechanism was not suitable to describe the measured data on P700 re-reduction kinetics while a tight binding mechanism led to good fits with rate constants in agreement with the literature.

It should be noted that the tight binding mechanism and the collisional mechanism are both simplifications. More generally, reactions should be described by the rates of binding (k_{on}), unbinding (k_o) and the internal electron transfer rate (k_3). However, no firm figures exist for plant cyt *bf* complexes. Therefore the simplifications of a tight binding and a collisional mechanism were introduced, reflecting two extreme cases.

Despite the simplifying assumptions about the reaction mechanism, our work clearly points out that the spatial organisation of the proteins within the thylakoid membrane may severely influence photosynthetic rate constants. Hence, more information about the thylakoid organisation is required. Furthermore, our results suggest that PQ oxidation at the Q_o site of cyt *bf* taking place in a heavily crowded membrane is expected to be reaction limited rather than diffusion limited. If a diffusion limited reaction were the case great differences between apparent (fractal) rate constants and rate constants found in dilute solutions *in vitro* are predicted. Unfortunately, data for rate constants of photosynthetic electron transport measured on isolated complexes are sparse and more data would be needed. However, isolated complexes may suffer the loss or modification of subunits and show severely artificial kinetics.

Acknowledgements

The authors wish to thank Dr. Thomas Strauß for the extended Powell-routine and countless helpful discussions about the software architecture and for his help with trouble shooting. Furthermore we wish to thank Dr. Alex Hope for helpful and interesting comments on an early stage of the manuscript. We also wish to thank the two anonymous reviewers for interesting and valuable comments.

The software for this work used the GAlib genetic algorithm package, written by Matthew Wall at the Massachusetts Institute

References

[1] B. Andersson, J.M. Anderson, Lateral heterogeneity in the distribution of chlorophyll–protein complexes of the thylakoid membranes of spinach chloroplasts, Biochim. Biophys. Acta 593 (1980) 427–440.

[2] J.M. Anderson, Insights into the consequences of grana stacking of thylakoid membranes in vascular plants: a personal perspective, Aust. J. Plant Physiol. 26 (1999) 625–639.

[3] L.A. Staehelin, M. DeWitt, Correlation of structure and function of chloroplast membranes at the supramolecular level, J. Cell. Biochem. 24 (1984) 261–269.

[4] J. Barber, Encyclopedia of Plant Physiology, New Series, Photosynthesis III, Ch. Surface Electrical Charges and Protein Phosphorylation, Springer Verlag, Berlin, 1986, pp. 653–664.

[5] P.-Å. Albertsson, The structure and function of the chloroplast photosynthetic membrane — a model for the domain organization, Photosynth. Res. 46 (1995) 141–149.

[6] P.-Å. Albertsson, The domain structure and function of the thylakoid membrane, Recent Res. Dev. Bioenerg. 1 (2000) 143–171.

[7] S.-G. Yu, G. Björn, P.-Å. Albertsson, Characterization of a non-detergent PSII- cytochrome b/f preparation (BS), Photosynth. Res. 37 (1993) 227–236.

[8] M.J. Saxton, Lateral diffusion in an archipelago. Distance dependence of the diffusion coefficient, Biophys. J. 56 (1989) 615–622.

[9] J. Lavergne, P. Joliot, Restricted diffusion in photosynthetic membranes, TIBS 16 (1991) 129–134.

[10] H. Kirchhoff, S. Horstmann, E. Weis, Control of the photosynthetic electron transport by PQ diffusion microdomains in thylakoids of higher plants, Biochim. Biophys. Acta, Bioenerg. 1459 (1) (2000) 148–168.

[11] I.G. Tremmel, H. Kirchhoff, E. Weis, G.D. Farquhar, Dependence of plastoquinol diffusion on the shape, size, and density of integral proteins, Biochim. Biophys. Acta 1607 (2003) 97–109.

[12] I.G. Tremmel, E. Weis, G.D. Farquhar, The influence of protein–protein interactions on the organisation of proteins within thylakoid membranes, Biophys. J. 88 (2005) 2650–2660.

[13] M.F. Blackwell, J. Whitmarsh, Examination of plastoquinone diffusion in lipid vesicles, Biophys. J. 58 (1989) 1259–1271.

[14] M.F. Blackwell, C. Gibas, S. Gygax, D. Roman, B. Wagner, The plastoquinone diffusion coefficient in chloroplasts and its mechanistic implications, Biochem. Biophys. Acta 1183 (1994) 533–543.

[15] R. Mitchell, A. Spillmann, W. Haehnel, Plastoquinol diffusion in linear photosynthetic electron transport, Biophys. J. 58 (1990) 1011–1024.

[16] M.J. Saxton, Chemically limited reactions on a percolation cluster, J. Chem. Phys. 116 (1) (2002) 203–208.

[17] R. Ellis, Macromolecular crowding: obvious but underappreciated, Trends 26 (10) (2001) 597–604.

[18] R. Ellis, A. Minton, Join the crowd, Nature 425 (2003) 27–28.

[19] H. Berry, Monte Carlo simulations of enzyme reactions in two dimensions: fractal kinetics and spatial segregation, Biophys. J. 83 (4) (2002) 1891–1901.

[20] A.P. Minton, The influence of macromolecular crowding and macromolecular confinement on biochemical reactions in physiological media, J. Biol. Chem. 276 (14) (2001) 10577–10580.

[21] W.L.C. Vaz, P.F.F. Almeida, Phase tolopogy and percolation in multi-phase lipid bilayers: is the biological membrane a domain mosaic? Curr. Opin. Struct. Biol. 3 (1993) 482–488.

[22] D. Hall, M.A.P., Macromolecular crowding: qualitative and semiquantitative successes, quantitative challenges, Biochim. Biophys. Acta 1649 (2) (2003) 127–139.

[23] G. Rivas, F. Ferrone, J. Herzfeld, Life in a crowded world, EMBO Rep. 5 (1) (2004) 23–27.

[24] B. Hankamer, J. Barber, E.J. Boekema, Structure and membrane organization of photosystem II in green plants, Annu. Rev. Plant Physiol. Plant Mol. Biol. 48 (1997) 641–671.

[25] C. Breyton, Conformational changes in the cytochrome b6f complex induced by inhibitor binding, J. Biol. Chem. 275 (2000) 13195–13201.

[26] W. Kühlbrandt, D.N. Wang, Three-dimensional structure of plant light-harvesting complex determined by electron crystallography, Nature 350 (1991) 130–134.

[27] H.H. Stiehl, H.T. Witt, Quantitative treatment of the function of plastoquinone in photosynthesis, Z. Naturforsch. 24 (1969) 1588–1598.

[28] W. Haehnel, The reduction kinetics of chlorophyll a_I as an indicator for proton uptake between the light reactions in chloroplasts, Biochim. Biophys. Acta 440 (1976) 506–521.

[29] P.J. Randall, D. Bouma, Zinc deficiency, carbonic anhydrase, and photosynthesis in leaves of spinach, Plant Physiol. 52 (1973) 229–232.

[30] H. Laasch, Non-photochemical quenching of chlorophyll *a* fluorescence in isolated chloroplasts under conditions of stressed photosynthesis, Planta 171 (1987) 220–226.

[31] H. Kirchhoff, Kontrolle des photosynthetischen Elektronentransportes in Thylakoiden höherer Pflanzen: Argumente fuer eine Mikrodomänenorganisation zwischen PS II und Cyt.b_6f Komplex., PhD thesis, Westfälische Wilhelms- Universität Münster (1998).

[32] A.B. Diner, V. Petrouleas, J.J. Wendoloski, The iron–quinone electron-acceptor complex of photosystem II, Physiol. Plant. 81 (1991) 423–436.

[33] P. Mitchell, Possible molecular mechanisms of the protonmotive function of cytochrome systems, J. Theor. Biol. 62 (1976) 327–367.

[34] B.L. Trumpower, The protonmotive Q cycle: coupling of proton translocation to electron transfer by the cytochrome bc1 complex., J. Biol. Chem. 265 (1990) 11409–11412.

[35] D.M. Kramer, A.R. Crofts, Current Research in Photosynthesis, Vol III, Kluwer, 1990, Ch. A Q-cycle mechanism for electron transfer in chloroplasts, pp. 283–286.

[36] D. M. Kramer, A. R. Crofts, Research in Photosynthesis, Vol II, Kluwer, 1993, Ch. A Q-cycle-type model for turn-over of the bf complex under a wide range of redox conditions., pp. 491–494.

[37] A.B. Hope, The chloroplast cytochrome *bf* complex: a critical focus on function, Biochim. Biophys. Acta 1143 (1993) 1–22.

[38] A.B. Hope, R.R. Huligol, M. Panizza, M. Thompson, D.B. Matthews, The flash induced turnover of cytochrome *b*-563, cytochrome *f* and plastocyanin in chloroplasts. Models and estimation of kinetic parameters, Biochim. Biophys. Acta 1100 (1992) 15–26.

[39] T. Link, The role of the 'Rieske' iron sulfur protein in the hydoquinone oxidation (Q_P) site of the cytochrome bc_1 complex. The proton gated mechanism, FEBS Lett. 412 (1997) 257–264.

[40] A.B. Diner, G.T. Babcock, Oxygenic photosynthesis: The light reactions, Kluwer Academic Publishers, 1996, Ch. 12. Structure, dynamics, and energy conversion efficiency in photosystem II., pp. 213–247.

[41] G. Hauska, G. Herold, C. Huber, W. Nitschke, D. Sofrova, Stigmatellin affects both hemes of cytochrome *b* in cytochrome *b6f/bc1*-complexes, Z. Naturforsch. 44c (1989) 462–467.

[42] A.R. Crofts, C.A. Wraight, The electrochemical domain of photosynthesis, Biochim. Biophys. Acta 726 (1983) 149–185.

[43] D.P. O'Keefe, Structure and function of the chloroplast cytochrome *bf* complex, Photosynth. Res. 17 (1988) 189–216.

[44] A.B. Hope, J. Liggins, D.B. Matthews, The kinetics of reactions in and near the cytochrome b/f complex of chloroplasts. II. cytochrome *b*-563 reduction, Aust. J. Plant Physiol. 16 (1989) 353–364.

[45] P. Joliot, A. Joliot, Electron transfer between the two photosystems: II. equilibrium constants, Biochim. Biophys. Acta 765 (1984) 219–226.

[46] F. Drepper, M. Hippler, W. Nitschke, W. Haehnel, Binding dynamics and electron transfer between plastocyanin and photosystem I, Biochemistry 35 (1996) 1282–1295.

[47] S. Berry, B. Rumberg, Kinetic modeling of the photosynthetic electron transport chain, Biochemistry 53 (2000) 35–53.

[48] M.J.D. Powell, An efficient method for finding the minimum of a function of several variables without calculating derivatives, Comput. J. 7 (1964) 155–163.

[49] W.H. Press, B.P. Flannery, S.A. Teukolsky, W.T. Vetterling, Numerical Recipes in C, The Art of Scientific Computing, Cambridge Univ. Press, 1998, pp. 309–317, (Ch. 10.5).

[50] P.R. Rich, P. Heathcote, D.A. Moss, Kinetic studies of electron transfer in a hybrid system constructed from the cytochrome *bf* complex and photosystem I, Biochim. Biophys. Acta 892 (1987) 138–151.
[51] W. Haehnel, Electron transport between plastoquinone and chlorophyll a_I in chloroplasts, Biochim. Biophys. Acta 305 (1973) 618–631.
[52] H. Kirchhoff, U. Mukherjee, H.-J. Galla, Molecular architecture of the thylakoid membrane: lipid diffusion space for plastoquinone, Biochemistry 41 (2002) 4872–4882.
[53] S.J. Jamieson, P. Wang, P. Qian, J.Y. Kirkland, M.J. Conroy, C.N. Hunter, P.A. Bullough, Projection structure of the photosynthetic reaction centre-antenna complex of *Rhodospirillum rubrum* at 8.5 Å resolution, EMBO J. 21 (2002) 3927–3935.
[54] S. Scheuring, J. Seguin, S. Marco, D. Levy, B. Robert, J.L. Rigaud, Nanodissection and high-resolution imaging of the *Rhodopseudomonas viridis* photosynthetic core complex in native membranes by AFM, Proc. Natl. Acad. Sci. 100 (2003) 1690–1693.
[55] D. Fotiadis, P. Qian, A. Philippsen, P.A. Bullough, A. Engel, C.N. Hunter, Structural analysis of the reaction center light-harvesting complex I photosynthetic core complex of *Rhodospirillum rubrum* using atomic force microscopy, J. Biol. Chem. 279 (1973) 2063–2068.
[56] F. Comayras, C. Jungas, J. Lavergne, Functional consequences of the organization of the photosynthetic apparatus in *Rhodobacter sphaeroides*: II. A study of PufX$^-$ membranes, J. Biol. Chem. 280 (2005) 11214–11223.
[57] M.J. Saxton, J.C. Owicki, Concentration effects on reactions in membranes: rhodopsin and transducin, Biochim. Biophys. Acta 979 (1989) 27–34.
[58] R. Kopelman, Fractal reaction kinetics, Science 241 (1988) 1620–1626.
[59] Y. Pierre, C. Breyton, C. Tribet, D. Kramer, J. Olive, P.J.L., Purification and characterization of the cytochrome b_6f complex from *Chlamydomonas reinhardtii*, J. Biol. Chem. 270 (1995) 29342–29349.
[60] B.-D. Hsu, A theoretical study on the fluorescence induction curve of spinach in the absence of DCMU, Biochim. Biophys. Acta 1140 (1992) 30–36.
[61] G. Hauska, M. Schütz, M. Büttner, Oxygenic Photosynthesis: The Light Reactions, Kluwer Academic Publishers, 1996, Ch. 19. The Cytochrome b_6f Complex-Composition, Structure and Function., pp. 377–398.
[62] W.A. Cramer, G.M. Soriano, M. Ponomarev, D. Huang, H. Zhang, S.E. Martinez, J.L. Smith, Some new structural aspects and old controversies concerning the cytochrome *b6f* complex of oxygenic photosynthesis, Annu. Rev. Plant Physiol. Plant Mol. Biol. 47 (1996) 477–508.